Bioorganic Chemistry 111 (2021) 104909

Contents lists available at ScienceDirect

Bioorganic Chemistry

journal homepage: www.elsevier.com/locate/bioorg

Synthesis, molecular modeling, selective aldose reductase inhibition and hypoglycemic activity of novel meglitinides

Manar G. Salem [a], Yasmine M. Abdel Aziz [a,*], Marwa Elewa [a,*], Mohamed S. Nafie [b], Hosam A. Elshihawy [a,*], Mohamed M. Said [a]

[a] Pharmaceutical Organic Chemistry Department, Faculty of Pharmacy, Suez Canal University, P.O. 41522 Ismailia, Egypt
[b] Chemistry Department, Faculty of Science, Suez Canal University, Ismailia 41522, Egypt

ARTICLE INFO

Keywords:
Meglitinides
Eparlestat
Repaglinide
ALR2
ALR1
SUR1

ABSTRACT

In the present study, a novel generation of selective aldose reductase ALR2 inhibitors with significant hypoglycemic activities was designed and modulated based on rhodanine scaffold joined to an acetamide linker in between two lipophilic moieties. The synthesis of the novel compounds was accomplished throughout simple chemical pathways. Molecular docking was performed on *B*-cell membrane protein SUR1, aldehyde reductase ALR1 and aldose reductase ALR2 active sites. Compounds **10B, 11B, 12B, 15C, 16C, 26F** and **27F** displayed the highest hypoglycemic activities with 80.7, 85.2, 87, 82.3, 83.5, 81.4 and 85.3% reduction in blood glucose levels, respectively. They were more potent than the standard hypoglycemic agent repaglinide with 65.4% reduction in blood glucose level. Compounds **12B** and **15C** with IC_{50} 0.29 and 0.35 μM were more potent than the standard ALR2 inhibitor epalrestat with IC_{50} 0.40 μM. They were selective towards ALR2 over ALR1 134 and 116 folds, respectively. Molecular docking studies matched with the *in-vitro* and *in-vivo* results to elucidate the dual activities of both compounds **12B** and **15C** as potent antagonists for ALR2 over ALR1 and good agonists for the SUR1 protein.

1. Introduction

Meglitinides are non-sulfonylureas hypoglycemic agents. They have the potential to stimulate pancreatic *B*-cells to secret more insulin and to improve insulin resistance in target tissues. It is well known that the pathological mechanisms of type 2 diabetes mellitus DM are mainly owing to reduced insulin secretion and insulin resistance in target tissues. As a result, meglitinides represent a single active treatment for type 2 DM with dual mechanisms of action [1]. Repaglinide (Fig. 1) is the most famous example of meglitinides. It is mainly metabolized in the liver and so it is safe for patients with renal impairment [2]. Repaglinide binds to site B of sulfonylurea receptor 1 SUR1 in pancreatic *B*-cells rather than site A that is targeted by sulfonylureas hypoglycemic agents such as gliclazide [3] (Fig. 1). Consequently, repaglinide has fast onset and duration of action. Thereby, it can normalize blood glucose level and eliminates the risk of drug-induced hypoglycemia. Despite all trials to develop novel hypoglycemic agents, long-term diabetic complications still life-threatening for diabetic patients [4]. Hyperglycemia stimulates the polyol pathway, triggering severe complications, such as cardiovascular disorders, kidney, eye and nerve damages. The main enzyme of the polyol pathway is aldose reductase ALR2 [5]. It is worth to mention that ALR2 has around 65% similarity in structure with aldehyde reductase ALR1 [6,7]. ALR1 is responsible for a crucial detoxification mechanism in human body [7]. Accordingly, the non-selective inhibition of both AR enzymes leads to serious adverse effects. Selective aldose reductase inhibitors ARIs such as epalrestat seem to be effective treatments for diabetic complications [6] with minimal undesirable effects. The recent study aimed to design a single drug, according to mixed pharmacophore theory, that can normalize glucose level in plasma and control chronic diabetic complications through selective ALR2 inhibition [8]. This was established through the modification of the only ARI approved drug, epalrestat (Fig. 2). In the present study, epalrestat scaffold was mainly modified according to three strategies. Strategy (A) was using simple lipophilic moieties attached to rhodanine core such as substituted benzylidene moieties in place of Baylise-Hillman adducts found in epalrestat structure [9]. Strategy (B) was keeping the rhodanine

* Corresponding authors.
E-mail addresses: yassmin_morsy@pharm.suez.edu.eg (Y.M. Abdel Aziz), marwa_elewa@pharm.suez.edu.eg (M. Elewa), hosamelshihawy74@hotmail.com (H.A. Elshihawy).

https://doi.org/10.1016/j.bioorg.2021.104909
Received 27 December 2020; Received in revised form 6 April 2021; Accepted 7 April 2021
Available online 20 April 2021

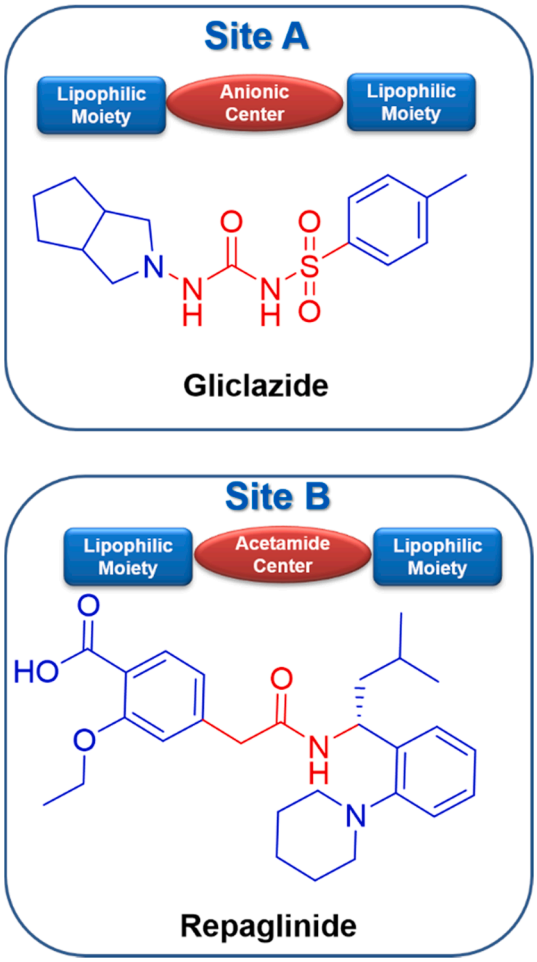

Fig. 1. Pharmacophoric model for gliclazide binding with site A and repaglinide binding with site B of SUR1.

moiety intact as it is essential for ARI activity. Strategy (C) involved the bioisosteric replacement of the carboxylic acid moiety of epalrestat with various substituted *N*-phenyl acetamide moieties. In this way, our designed structures fulfill the minimum pharmacophoric criterion for improving hypoglycemic activity which is the presence of acetamide moiety in between two lipophilic centers [10]. This acetamide moiety ionizes at the physiological pH to give an anionic center that plays a crucial role in enhancing the binding affinity to SUR1 [10]. This study aimed to the synthesis of 7 Series (**A-G**) of novel hypoglycemic compounds as well as selective ALR2 inhibitors, inspired by epalrestat [11] and repaglinide structures, throughout simple chemical pathways [12] (Fig. 2).

2. Results and discussion

2.1. Chemistry

Scheme I illustrated the synthetic route developed for the synthesis of 4 intermediate compounds, 2-chloro-*N*-phenylacetamide derivatives **3(A-D)**, through the reaction of chloroacetyl chloride with various aniline derivatives **2(A-D)** in glacial acetic acid at 100 °C [13,14]. Scheme II involved the synthesis of 5-arylidenerhodanine compounds **5(A-G)** through the addition of 2-thioxothiazolidin-4-one, different aldehydes **4 (A-G)** and anhydrous sodium acetate in glacial acetic acid [9,11]. Scheme III showed the synthesis of acetamide derivatives of 5-arylidenerhodanine compounds [series (**A-G**] through the addition of sodium bicarbonate and sodium iodide to 5-arylidenerhodanine compounds **5 (A-G)** and intermediate compounds, 2-chloro-*N*-phenylacetamide derivatives **3(A-D)** in DMF [15]. The target compounds [series (**A-G**] were synthesized via the simplest and the most economic chemical pathway.

Microanalyses and spectral data (IR, ^{1}H NMR, ^{13}C NMR and EI-MS) were used to elucidate the structure of the synthesized compounds **6A-33G**. The IR Spectra for Series **A** and **G** showed collectively NH and C═O stretching at around 3300–3500 cm^{-1} and 1630–1700 cm^{-1} respectively, the appearance of (Ar-H, sp^{2}) stretching at 3000–3100 cm^{-1}, (=C—H) stretching at 3010–3100 cm^{-1}, (C—H, sp^{3}, alkyl) stretching at 2850–3000 cm^{-1}, overtones weak bands at 2000–1665 cm^{-1}, (*N*-C═O) at around 1665–1710 cm^{-1}, (Ar C═C) stretching at around 1450–1600 cm^{-1} and (*N*-C═S) at around 1025–1225 cm^{-1}. Besides, the appearance of (O-CH$_3$, ether) stretching at 1150 cm^{-1} and 1170 cm^{-1} in compounds **8A** and **32G** respectively. On the other hand, the IR spectra for series **B** and **F** illustrated the same bands as series **A** except for (O-CH$_3$, ether) stretching at 1050–1250 cm^{-1}. IR Spectra of series **C** showed same bands as series **A** except for (O—H) stretching at 3200–3400 cm^{-1} and (C—O, alcoholic) stretching at around 1050–1250 cm^{-1}. Concerning series **D**, (C—N, amine) stretching appeared at 1080–1360 cm^{-1}. In series **E**, two strong stretching related to (N—O, nitro) were observed at 1515–1560 and 1345–1385 cm^{-1}. ^{1}H NMR spectra of the newly synthesized compounds of series **(A-G)** showed NH singlets at δ_H [9.76–10.50 ppm]. Besides, the proton of the methylidene group (=C—H) appeared as downfield singlets at δ_H [7.30–8.63 ppm]. ^{1}H NMR Spectra were characterized by two important regions: a highly shielded region consisting of aliphatic characteristic signals corresponding to methylene of acetamide moiety at δ_H [3.82–4.50 ppm] and a deshielded region consisting of aromatic multiplets corresponding to substituted phenyl and substituted benzylidene rings at δ_H [6–8.5 ppm]. In addition, in series **B** and **F**, singlets at δ_H [3–3.5 ppm] were observed that referred to the three protons of methoxy group (O-CH$_3$). Regarding the ^{1}H NMR spectra of series **C**, singlets at δ_H [10–10.5 ppm] were detected that referred to the hydroxyl group (OH). Compounds of series **D** obtained dimethylamino group (N-(CH$_3$)$_2$) that was observed as singlets at δ_H [3–3.5 ppm] that referred to six equivalent protons. The ^{13}C NMR spectra showed characteristic decoupled signals for 5-benzylidene rhodanine, phenyl rings and acetamide moiety at the expected regions. In the rang δ_C [160–195 ppm] several characteristic peaks were observed that referred to (C═S), (C═O, acetamide) and (C═O, rhodanine). Besides, the aromatic carbons were observed at δ_C [111–158 ppm]. Aliphatic carbons of (methylene group of acetamide, methoxy group and dimethylamino group) were elucidated at δ_C [40–55 ppm].

2.2. Biological activity

In-vivo hypoglycemic activity of novel compounds was evaluated. In addition, the potential inhibitory activity against ALR1 and ALR2 enzymes as well as selectivity indices were determined. Most of the screened compounds might serve as suitable candidates to treat diabetes and diabetic complications by using a single medication with dual activity.

2.2.1. In-vivo hypoglycemic activity

The *in-vivo* studies for compounds of series **(A-G)** representing meglitinide were performed on BALB/c mice. Diabetes was induced, the blood samples were collected at time intervals 0, 2, 4, 6 and 8 h and the blood glucose levels were measured. The results are listed in Table 1.

Most of the tested compounds of series **(A-G)** possessed potent glucose lowering activities as hypoglycemic agents. Compounds **10B, 11B, 12B, 15C, 16C, 26F** and **27F** displayed the highest activities with 80.7, 85.2, 87, 82.3, 83.5, 81.4 and 85.3% reduction in blood glucose levels, respectively. They were more potent than **standard 2** with 65.4% reduction and comparable to **standard 1**. It was observed that these compounds of series **B, C** and **F** obtained methoxy and hydroxyl substituents on the benzylidene rhodanine moiety. Compounds of series **D** and **E**, with N, *N*-dimethyl amino and nitro substituents at p-position of

the benzylidene rhodanine moiety respectively, obtained moderate activities with 75.9–62.3% reduction. Both of series **A** and **G** exhibited weak hypoglycemic activities. Compounds **7A** and **33G** displayed the lowest activity. This might be attributed to the absence of o- or p-substitution on benzylidene rhodanine moiety.

2.2.2. ALR1 and ALR2 activity

Inhibitory activities of the novel compounds were screened *in-vitro* against ALR1 and ALR2 using UV spectrophotometer on the basis of measuring the decrease in the UV absorption by NADPH at 340 nm [16]. The positive control was valproic acid for ALR1 [10] and epalrestat for ALR2 [9]. The results are listed in Table 2.

Among the 7 series, series **B** was the most active one as potent inhibitor for ALR2 with exciting selectivity index. Compounds **12B** and **15C** with IC_{50} 0.29 and 0.35 μM were more potent than epalrestat, with IC_{50} 0.40 μM. They were selective towards ALR2 over ALR1 134 and 116 folds, respectively. This therapeutic potential might be attributed to the presence of 4-OCH_3 and 2-OH substituents attached to the benzylidene moiety in addition to 4-OCH_3 and 2,4-diCl attached to the phenyl ring in compounds **12B** and **15C**, respectively. On the other hand, the replacement of methoxy substituent at *para*-position on benzylidene moiety by the same one at *meta*-position of arylidene moiety in series **F** render the compounds very weak than their analogs in series **B**. Regarding series **C,** the presence of a hydroxyl substituent at *ortho*-position slightly affected the activity of the compounds as inhibitors for ALR2. Therefore, the compounds of series **C** were still active inhibitors compared to the standard. Moreover, the compounds of series **D** and **E** obtained moderated potencies and IC_{50} of 0.94 to 8.42 μM. Compounds

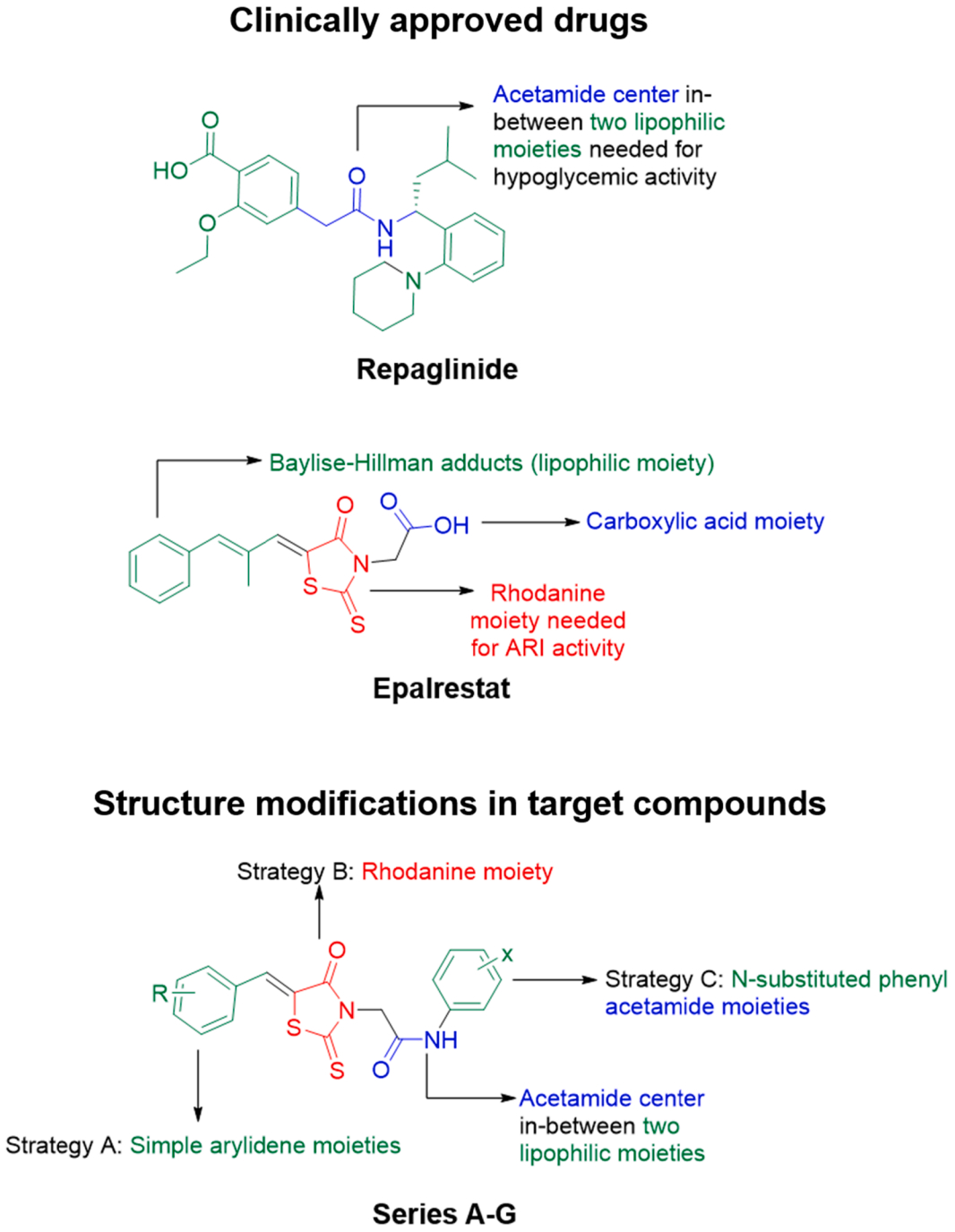

Fig. 2. The proposed scaffolds of hypoglycemic agents [series (A-G)].

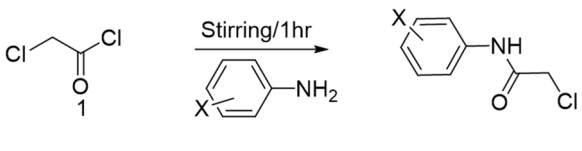

2(A-D) 3(A-D)

Compd.	X
2A	4-Br
2B	2,4-diCl
2C	4-OCH_3
2D	4-Cl

Compd.	X
3A	4-Br
3B	2,4-diCl
3C	4-OCH_3
3D	4-Cl

Scheme I. Synthesis of 2-chloro-*N*-arylacetamide derivatives (intermediates) 3 (A-D).

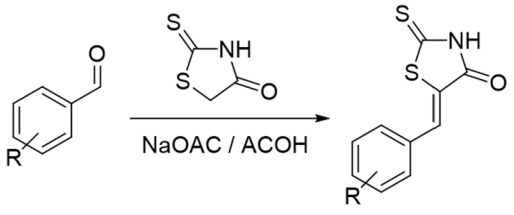

4(A-G) 5(A-G)

Compd.	R
4A	4-H
4B	4-OCH_3
4C	2-OH
4D	4-N-$(CH_3)_2$
4E	4-NO_2
4F	3-OCH_3
4G	4-Br

Compd.	R
5A	4-H
5B	4-OCH_3
5C	2-OH
5D	4-N-$(CH_3)_2$
5E	4-NO_2
5F	3-OCH_3
5G	4-Br

Scheme II. Synthesis of 5-arylidenerhodanine compounds (intermediates) 5 (A-G).

of **D** and **E** series obtained N, *N*-dimethyl amino and nitro substituents at *para*-position on benzylidene moiety respectively. The weakest compounds were in series **A**, **F** and **G**. These series obtained no substitution (series **A**) or contained m-substituents on benzylidene ring (series **F** and **G**) which resulted in a decreased interaction with the active site of ALR2.

2.2.3. The selectivity indices of the novel compounds

The selective inhibition of the novel compounds was calculated in terms of their IC_{50} values against ALR1 versus ALR2. In all series, remarkable selectivity indices were observed for compounds **10B, 11B**, **12B**, **15C** and **22E** with 39, 45, 134, 116 and 38 folds, respectively. These compounds were more selective towards ALR2. Therefore, compounds of series **B** might be considered potent and selective inhibitors with minor side effects. According to the previous three parameters, *in-vivo* hypoglycemic activity, *in-vitro* ALR1 and ALR2 inhibitory activity and the selectivity indices of the novel compounds, the most active compounds were **12B** and **15C**.

2.3. In silico studies

2.3.1. Molecular modeling

Molecular docking study was performed to rationalize the *in-vivo* and *in-vitro* biological results and give insights into the possible binding modes of compounds of the **7** series (**A-G**) together with the co-crystallized ligands within the active sites of 6PZ9 (SUR1), aldose reductase (4QR6) and aldehyde reductase enzymes (3H4G).

Among the highest active compounds **12B** and **15C** were highlighted for their binding mode inside the 4QR6 (ALR2) and 3H4G (ALR1) to elucidate their over selectivity towards the ALR2 over the AlR1. As seen in Table 3**,** compound **12B** was docked inside the 4QR6 with a strong binding energy −24.11 Kcal/mol, it formed 2H-bonds with His 110, and Trp 111 and two arene-arene with Tyr 209 and Trp 111 as the co-crystallized ligand NADP, but it was docked inside the 3H4G with lower binding energy −11.2 Kcal/mol, and it did not form any interactive hydrogen bond (H-bond) like NADP, it only formed week interactions of one arene-arene with Trp 22**.** While compound **15C,** was docked inside the 4QR6 with a good binding energy −16.43 Kcal/mol, it formed 2H-bonds with His 110, and Tyr 48 and One arene-arene with Trp 20 as the co-crystallized ligand NADP, but it was docked inside the 3H4G with lower binding energy −11.9 Kcal/mol, and it did not form any interactive H-bond like NADP, it only formed week interactions of one arene-arene interaction with Trp 22.

Moreover, as seen in Fig. 3**A,** it was noticed that ligand **12B** tightly bounded itself inside the binding site by two distinct H-bonds with His110 (with bond length 1.72 Å) and Trp11 (with bond length 1.45 Å) through the oxygen atoms as H-bond acceptors of rhodamine and acetamide, respectively. Also, compound **15C**, as seen on Fig. 3**B,** tightly bounded itself inside the binding site by two strong H-bonds with His110 (with bond length 1.82 Å) and Tyr48 (with bond length 2.06 Å) through the oxygen atom as H-bond acceptor acetamide. These strong H-bond interactions were deterministic in targeting ALR2. In addition, it showed significant interactions with both polar and hydrophobic residues of ALR2 that further increased its binding affinity.

So, from the strong interactive binding modes of the two docked compounds inside the two rested proteins, we could conclude the over selectivity against the 4QR6 over 3H4G, this in agreement with the *in-vitro* inhibitory biological results of both compound **12B** and **15C** towards ALR2 with IC_{50} of 0.29 and 0.35 μM, respectively compared to Epalrestate (IC_{50} = 0.40 μM) and AlR1 with IC_{50} of 39.11 and 40.72 μM, respectively compared to Valproic acid (IC_{50} = 57.4 μM).

To predict the mode of action of the docked compounds **12B** and **15C** compared with the co-crystallized ligand (Repaglinide), they were evaluated as agonists for their binding affinities towards the molecular target (PDB: 6PZ9) as a SUR1 membrane protein in pancreatic B-cell to stimulate insulin secretion [18]. As seen in Table 4 with the two- and three-dimensional representation of the overall interaction inside the binding site of the target molecule, compound **12B** was docked inside the receptor binding site with binding energy –22.63 Kcal/mol, to form **2**H-bonds with Asn 437 (bond length 2.16 Å) and Arg 1248 (1.75 Å) as H-bond acceptors through (–OCH_3) substituents and C═O group of acetamide group, respectively. While compound **15C**, was docked inside the receptor binding site with binding energy −21.41 Kcal/mol, to form 1H-bonds with Asn 437 (bond length 2.34 Å) as H-bond acceptor through C═O group of acetamide group.

So, the molecular docking study elucidates the feasible mechanism of binding of both compounds **12B** and **15C** to act as agonist inside the 6PZ9 (SUR1) protein, which explains their high biological activity as a hypoglycemic agent (87% and 82.3% reduction in blood glucose, respectively).

3. Bioinformatics study

Bioinformatics studies were conducted to establish physicochemical properties and drug-like properties for compounds **10B**, **11B**, **12B**, **15C**, **16C**, **26F** and **27F** that exhibited the most potent hypoglycemic activities. The examined compounds showed promising drug-likeness grads and good physicochemical properties according to Lipinsiki's rule of five [17]. These physicochemical properties included molecular weight, number of rotatable bonds, H-bond donor and acceptors along with number of violations. Furthermore, acceptable pharmacokinetics such as permeability and intestinal absorption were observed too. For good drug absorbance through intestine, the value of topological polar surface area (TPSA) should be as low as 140. Blood brain barrier (BBB) should be as low as 90 $Å^2$ [18]. The examined compounds showed good absorption and permeability. As shown in Table 5, the tested compounds had 1–2H-bond donors and 5–6H-bond acceptors. Besides, all tested compounds

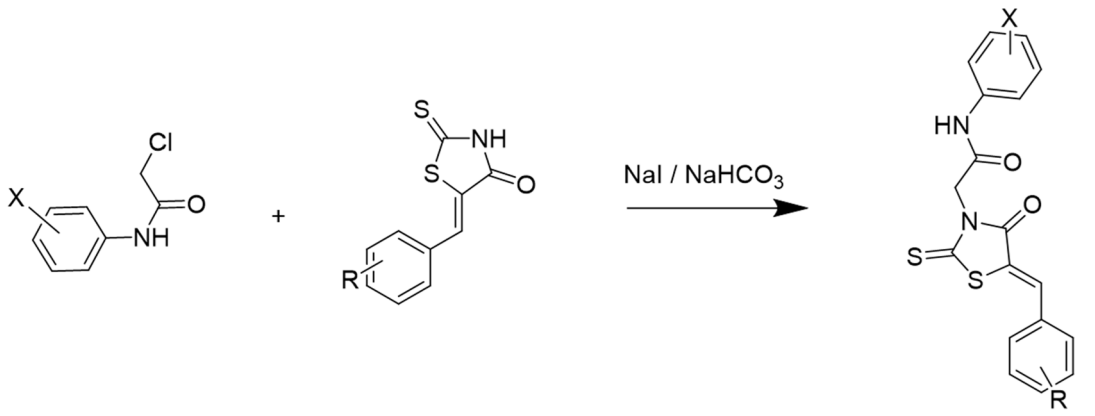

3(A-D) 5(A-G) Series A - G (6A-33G)

Compd.	X
3A	4-Br
3B	2,4-diCl
3C	4-OCH_3
3D	4-Cl

Compd.	R
5A	4-H
5B	4-OCH_3
5C	2-OH
5D	4-N-$(CH_3)_2$
5E	4-NO_2
5F	3-OCH_3
5G	4-Br

Compd.	X	R
6A	4-Br	H
7A	2,4-Cl	H
8A	4-OCH_3	H
9A	4-Cl	H
10B	4-Br	4-OCH_3
11B	2,4-Cl	4-OCH_3
12B	4-OCH_3	4-OCH_3
13B	4-Cl	4-OCH_3
14C	4-Br	2-OH
15C	2,4-Cl	2-OH
16C	4-OCH_3	2-OH
17C	4-Cl	2-OH
18D	4-Br	4-$N(CH_3)_2$
19D	2,4-Cl	4-$N(CH_3)_2$
20D	4-OCH_3	4-$N(CH_3)_2$
21D	4-Cl	4-$N(CH_3)_2$
22E	4-Br	4-NO_2
23E	2,4-Cl	4-NO_2
24E	4-OCH_3	4-NO_2
25E	4-Cl	4-NO_2
26F	4-Br	3-OCH_3
27F	2,4-Cl	3-OCH_3
28F	4-OCH_3	3-OCH_3
29F	4-Cl	3-OCH_3
30G	4-Br	3-Br
31G	2,4-Cl	3-Br
32G	4-OCH_3	3-Br
33G	4-Cl	3-Br

Scheme III. Synthesis of the final compounds.

exhibited log P values between 2.69 and 4.04, so they were well tolerated through cellular membranes. For controlling oral bioavailability and conformational changes, the rotatable bond number (nrotb) should be ≤10 [19]. All the tested compounds had 4–6 nrotb. Additionally, compounds **12B** and **15C,** exhibited good gastrointestinal tract absorption according to the BOILED-Egg model as shown in Fig. 4. Consequently, these compounds could be considered drug-like candidates. The dual activity of the designed molecules as hypoglycemic agents as well as selective ALR2 inhibitors based on the observed structure–activity relationships (SAR) were summarized in Fig. 5.

4. Experimental

4.1. Materials and methods for synthesis and analytical characterization

"All reagents were purchased from Aldrich, Merck and Fluka and were used without any further purification. Melting points were measured on an electrothermal apparatus in open capillary tubes using Stuart melting point apparatus SMP10 and were uncorrected. Infrared (IR) spectra were measured using KBr discs on a Vector 22 Infrared spectrophotometer (υ_{max} in cm^{-1}), with ratio (1drug: 3 KBr). Nuclear Magnetic Resonance spectra were recorded on Bruker spectrometer (400 MHz). Electron impact mass spectra (EI-MS) were recorded on a Finnigan MAT 312 mass spectrometer connected with a MASPEC Data System. Elemental analyses were performed in the Microanalytical center, Al Azhar University, Egypt".

4.1.1. 2-Chloro-N-Arylacetamide derivatives 3(A-D)

Aniline derivatives **3(A-D)** (24.4 mmol) were dissolved in glacial acetic acid (15 mL). Chloroacetyl chloride (25.1 mmol, 2.0 mL) was added dropwise to the mixture. The reaction mixture was stirred and heated at reflux for 1 h. The completion of reaction was monitored using TLC (*n*-hexane/ AcOEt = 3:2). After completion of reaction, the mixture was cooled to RT. Sodium acetate solution (0.4 M, 39 mL) was added

Table 1
Blood glucose concentration (mg/dl) in diabetic mice treated with series (A-G) compounds.

Comp. codes	Glucosemg/dl basal	Glucosemg/dlAfter 2 h	Glucosemg/dlAfter 4 h	Glucosemg/dlAfter 6 h	Glucosemg/dlAfter 8 h	Inhibition after8 h (%)
6A	358 ± 6.98	310 ± 6.84	283 ± 7.18	221 ± 4.71	127 ± 5.25	64.5
7A	321 ± 5.75	266 ± 7.34	197 ± 9.32	221 ± 2.61	274 ± 8.45	———
8A	361 ± 6.98	304 ± 8.84	253 ± 7.40	236 ± 4.78	159 ± 2.45	55.9
9A	398 ± 8.23	317 ± 7.93	282 ± 5.57	221 ± 4.91	149 ± 5.33	62.6
10B	436 ± 3.56	352 ± 5.54	237 ± 4.71	184 ± 6.58	74 ± 2.83	80.7
11B	461 ± 5.93	347 ± 5.62	240 ± 6.16	165 ± 2.75	68 ± 5.13	85.2
12B	485 ± 4.82	376 ± 7.01	281 ± 4.74	184 ± 5.22	63 ± 4.45	87
13B	441 ± 7.73	319 ± 7.41	269 ± 5.46	217 ± 6.30	105 ± 4.42	76.1
14C	384 ± 3.71	340 ± 5.67	233 ± 4.61	121 ± 4.89	100 ± 3.45	73.9
15C	413 ± 4.14	320 ± 4.82	295 ± 6.43	229 ± 5.74	73 ± 4.63	82.3
16C	456 ± 3.57	253 ± 3.78	223 ± 5.08	185 ± 4.82	75 ± 3.17	83.5
17C	373 ± 3.18	315 ± 5.33	235 ± 8.46	181 ± 5.11	93 ± 8.45	75.1
18D	395 ± 3.39	316 ± 3.65	282 ± 3.59	214 ± 2.14	113 ± 1.54	71.3
19D	384 ± 4.76	312 ± 4.88	254 ± 5.43	195 ± 1.87	131 ± 4.78	65.8
20D	381 ± 4.66	289 ± 5.98	227 ± 3.43	193 ± 1.17	98 ± 4.78	74.2
21D	353 ± 5.67	261 ± 3.98	214 ± 5.54	284 ± 5.87	155 ± 3.12	56.1
22E	366 ± 5.89	271 ± 6.37	213 ± 4.23	184 ± 6.98	131 ± 2.36	64.2
23E	401 ± 4.34	352 ± 4.24	281 ± 5.43	223 ± 1.87	151 ± 4.58	62.3
24E	429 ± 4.77	331 ± 3.52	222 ± 3.82	181 ± 6.33	103 ± 2.87	75.9
25E	390 ± 5.43	325 ± 5.74	257 ± 7.51	189 ± 7.31	125 ± 3.17	67.9
26F	458 ± 7.93	364 ± 7.58	261 ± 9.22	213 ± 4.71	85 ± 5.89	81.4
27F	470 ± 7.69	338 ± 6.34	252 ± 3.12	115 ± 2.96	69 ± 3.36	85.3
28F	391 ± 6.43	278 ± 8.34	230 ± 5.46	194 ± 7.31	118 ± 2.44	69.8
29F	399 ± 7.19	265 ± 4.67	194 ± 3.82	134 ± 3.69	91 ± 2.43	77.2
30G	377 ± 4.55	293 ± 8.34	202 ± 5.36	189 ± 7.42	132 ± 2.41	649
31G	350 ± 4.56	291 ± 4.98	216 ± 5.43	187 ± 1.87	149 ± 4.78	57.4
32G	362 ± 6.75	275 ± 7.55	219 ± 9.36	192 ± 2.61	161 ± 8.45	55.5
33G	386 ± 5.67	272 ± 3.98	249 ± 5.88	275 ± 5.84	360 ± 3.81	———
Standard 1[a]	459 ± 3.88	386 ± 7.01	276 ± 4.54	182 ± 7.22	69 ± 4.77	85.1
Standard 2[b]	368 ± 4.66	302 ± 5.22	279 ± 3.75	198 ± 4.43	127 ± 1.86	65.4

a) **Standard 1** is the reported compound N-(2,4-Dichlorophenyl)-2-(2′,4′- dioxospiro[fluorene-9,5′-imidazolidine]-3′-yl)acetamide by M.G.Salem et al. [3].
b) **Standard 2** is repaglinide.
Values represent mean ± SEM.

subsequently. The mixture was stirred in an ice bath for 5 min [14] [1 1 5]. The formed precipitate was filtered, washed with water and recrystallized from methanol to yield compounds **3(A-D)**.

4.1.2. 2-Chloro-N-(4-Bromophenyl) acetamide 3A
White crystals, M.p. 180–182, yield 95% [23].

4.1.3. 2-Chloro-N-(2,4-dichlorophenyl) acetamide 3B
White needle crystals, M.p. 106–108, yield 99% [24].

4.1.4. 2-Chloro-N-(4-methoxyphenyl) acetamide 3C
Yellow white crystals, M.p. 61, yield 88% [25].

4.1.5. 2-Chloro-N-(4-chlorophenyl) acetamide 3D
White needle crystals, M.p. 169–171, yield 83%[15].

4.1.6. 5-Arylidenerhodanine compounds 5(A-G)
A mixture of rhodanine (3 mmol), different aldehydes (3 mmol) and anhydrous sodium acetate (3 mmol) were taken in glacial acetic acid (10 mL). The reaction mixture was heated to 120 °C in oil bath for 3–4 h. The reaction was monitored by TLC (*n*-hexane/ AcOEt = 3:2). Upon completion, the reaction mixture was cooled and the formed precipitate was filtered, washed with water and recrystallized from methanol to yield compounds (**5A-5G**) [9,26–28].

4.1.7. 5-Benzylidene-2-thioxothiazolidin-4-one 5A
Yellow crystalline solid, m.p. (203–205) °C, yield 90% [29,30].

4.1.8. 5-(4-Methoxybenzylidene)-2-thioxothiazolidin-4-one 5B
Yellow crystalline solid, m.p. (260–262) °C, yield 90% [29,31].

4.1.9. 5-(2-Hydroxybenzylidene)-2-thioxothiazolidin-4-one 5C
Yellow crystalline solid, m.p. (223–225) °C, yield 83% [29].

4.1.10. 5-(4-(Dimethylamino)benzylidene)-2-thioxothiazolidin-4-one 5D
Orange crystalline solid, m.p. (284–286) °C, yield 90% [29,31].

4.1.11. 5-(4-Nitrobenzylidene)-2-thioxothiazolidin-4-one 5E
Yellowish orange crystalline solid, m.p. (254–256) °C, yield 98% [32,30,31,28].

4.1.12. 5-(3-Methoxybenzylidene)-2-thioxothiazolidin-4-one 5F
Yellow crystalline solid, m.p. (236–238) °C, yield 80% [29].

4.1.13. 5-(3-Bromobenzylidene)-2-thioxothiazolidin-4-one 5G
Yellow crystalline solid, m.p. (243–245) °C, yield 70% [29].

4.1.14. 2-(5-Arylidene-4-oxo-2-thioxothiazolidin-3-yl)-N-(substituted phenyl) acetamide series (A-G)
Sodium bicarbonate (2.36 mmol) and sodium iodide (2.36 mmol) were added to a solution of compounds **3(A-D)** (2.36 mmol) and compounds **5(A-G)**, (2.36 mmol) in DMF (30 mL). The reaction mixture was stirred at RT for 36 hrs. The mixture was then poured into water (50 mL) to afford the desired product. The precipitate was filtered and recrystallized from absolute ethanol [15].

4.1.15. Z-N-(4-Bromophenyl)-2-(5-benzylidene-4-oxo-2-thioxothiazolidin-3-yl)acetamide 6A
Yellow crystals; yield 76%; m.p.; (110–113) °C; IR (KBr, cm^{-1}): 3245, 3090, 2856, 1705, 1543, 1205; EI-MS (*m/z*, %): 432 (M^+), 433 (M^++1), 434 (M^++2); ^{1}H NMR (400 MHz) (DMSO): δ_H 10.68 (s, 1H), 8.28–8.17 (m, 2H) 7.88 (s, 1H), 7.79 (d, ^3J = 8 Hz, 2H), 7.58–7.37 (m, 5H), 4.16 (m, 2H); ^{13}CNMR (DMSO-d_6): δ_C 48.9, 116.7, 122.5, 127.4, 127.7, 128.1, 129.1, 131.2, 132.1, 134.2, 138.4, 164.2, 165.4, 190.8. Anal. Calcd. for $C_{18}H_{13}BrN_2O_2S_2$: C, 49.89; H, 3.02; N, 6.46. Found: C, 49.94; H, 3.43; N, 6.57.

Table 2
In-vitro inhibitory activities of the compounds of series (**A-G**) against ALR1 and ALR2.

Comp. codes	ALR1	ALR2	S. E
	IC_{50} ± SEM (μM)[I]/(Inhibition %)		IC_{50}[ALR1]/ IC_{50}[ALR2]
6A	19.54 ± 0.32	20.43 ± 0.14	0.95
7A	12.81 ± 0.05	10.42 ± 2.07	1.22
8A	26.55 ± 0.89	30.91 ± 0.02	0.86
9A	22.93 ± 0.98	41.62 ± 0.11	0.55
10B	18.53 ± 0.07	0.47 ± 0.13	39.3
11B	19.72 ± 0.63	0.43 ± 0.12	45.8
12B	39.11 ± 1.71	0.29 ± 0.10	134
13B	11.23 ± 0.16	1.51 ± 0.08	7.43
14C	14.51 ± 0.23	0.78 ± 0.07	18.6
15C	40.72 ± 0.61	0.35 ± 0.08	116
16C	27.2 ± 1.42	0.64 ± 0.26	22.8
17C	10.11 ± 0.72	1.04 ± 0.02	9.71
18D	17.82 ± 0.28	1.98 ± 0.31	8.99
19D	16.23 ± 1.45	3.09 ± 0.06	5.24
20D	9.18 ± 0.05	2.41 ± 2.07	3.80
21D	11.33 ± 1.42	8.42 ± 0.03	1.34
22E	35.92 ± 1.87	0.94 ± 0.77	38.2
23E	13.25 ± 1.03	2.87 ± 0.18	4.61
24E	22.82 ± 0.54	1.52 ± 1.06	15.0
25E	17.67 ± 2.51	7.13 ± 0.86	2.47
26F	12.21 ± 0.06	7.36 ± 0.08	1.65
27F	18.43 ± 1.13	10.47 ± 0.28	1.76
28F	11.86 ± 0.05	12.12 ± 1.14	0.97
29F	15.54 ± 0.89	18.15 ± 0.02	0.85
30G	17.66 ± 0.13	13.54 ± 0.01	1.28
31G	25.58 ± 0.97	14.96 ± 0.16	1.72
32G	19.05 ± 0.73	21.18 ± 2.07	0.93
33G	5.39 ± 0.68	8.62 ± 0.06	0.67
Valproic acid	57.4 ± 0.89[II]	–	–
Epalrestate	–	0.40[III]	–

I: n = Values are expressed as "Mean ± SEM" of three independent trials.
II: IC_{50} of Valproic acid 56.1 ± 2.7 μM reported by Stefek et al. [16].
III: IC_{50} of epalrestat reported by T.N. Reddy et al. [9].

4.1.16. Z-N-(2,4-Dichlorophenyl)-2-(5-benzylidene-4-oxo-2-thioxothiazolidin-3-yl)acetamide 7A

Yellow crystals; yield 68%; m.p. (121–123) °C; IR (KBr, cm^{-1}): 3245, 3041, 2870, 1660, 1547, 1200; EI-MS (*m/z*, %): 422 (M^+), 423 (M^++1), 424 (M^++2); ^{1}H NMR (400 MHz) (DMSO): δ_H 9.49 (s, 1H), 7.86 (d, ^4J = 1.52 Hz, 1H), 7.73 (s, 1H), 7.64–7.57 (m, 3H), 7.50–7.47 (m, 2H), 7.40–7.38 (m, 2H), 4.51 (s, 2H); ^{13}CNMR (DMSO-d_6): δ_C 48.6, 122.5, 123.6, 127.2, 128.5, 129.1, 129.4, 131.0, 133.6, 134.9, 138.8, 164.2, 165.1, 191.1. Anal. Calcd. for $C_{18}H_{12}Cl_2N_2O_2S_2$: C, 51.07; H, 2.86; N, 6.62. Found: C, 51.50; H, 3.13; N, 6.88.

4.1.17. Z-N-(4-Methoxyphenyl)-2-(5-benzylidene-4-oxo-2-thioxothiazolidin-3-yl)acetamide 8A

Brown crystals; yield 70%; m.p. (93–95) °C; IR (KBr, cm^{-1}): 3364, 3023, 2911, 1707, 1570, 1204, 1150; EI-MS (*m/z*, %): 384 (M^+), 385 (M^+ +1); ^{1}H NMR (400 MHz) (DMSO): δ_H 10.45 (s, 1H), 7.96 (s, 1H), 7.47 (d, ^3J = 7.9 Hz, 2H), 7.37 (d, ^3J = 7.9 Hz, 2H), 7.20–6.97 (m, 5H), 4.04 (m, 2H), 3.72 (s, 3H); ^{13}CNMR (DMSO-d_6): δ_C 45.5, 55.19, 111.2, 122.9, 127.2, 128.9, 129.4, 130.2, 134.1, 134.7, 136.7, 157.5, 165.5, 166.7, 189.4. Anal. Calcd. for $C_{19}H_{16}N_2O_3S_2$:. C, 59.36; H, 4.19; N, 7.29. Found: C, 58.89; H, 4.58; N, 7.71.

4.1.18. Z-N-(4-Chlorophenyl)-2-(5-benzylidene-4-oxo-2-thioxothiazolidin-3-yl)acetamide 9A

Dark brown; yield 73%; m.p. (105–107) °C; IR (KBr, cm^{-1}): 3396, 3055, 2889, 1652, 1568, 1211; EI-MS (*m/z*, %): 388 (M^+), 389 (M^++1), 390 (M^++2); ^{1}H NMR (400 MHz) (DMSO): δ_H 9.99 (s, 1H), 7.52–7.31 (m, 5H), 7.31 (d, ^3J = 7.8 Hz, 2H), 7.08 (s, 1H), 6.75 (d, ^3J = 7.8 Hz, 2H), 4.51 (s, 2H). ^{13}CNMR (DMSO-d_6): δ_C 48.9, 121.3, 122.5, 127.6, 128.1, 128.8, 129.5, 131.3, 132.2, 135.1, 138.8, 164.4, 165.1, 191.0. Anal. Calcd. for $C_{18}H_{13}ClN_2O_2S_2$: C, 55.59; H, 3.37; N, 7.20. Found: C, 55.92; H, 3.65; N, 7.66.

4.1.19. Z-N-(4-Bromophenyl)-2-(5-(4-methoxybenzylidene)-4-oxo-2-thioxothiazolidin-3-yl)acetamide 10B

Dark yellow; yield 67%; m.p. (132–134) °C. IR (KBr, cm^{-1}): 3259, 3016, 2890, 1681, 1548, 1223, 1073; EI-MS (*m/z*, %): 462 (M^+), 463 (M^++1), 464 (M^++2). ^{1}H NMR (400 MHz) (DMSO): δ_H 10.26 (s, 1H), 7.53 (d, ^3J = 8.2 Hz, 2H), 7.39 (d, ^3J = 7.7 Hz, 2H), 7.21 (d, ^3J = 8.2 Hz, 2H), 7.15 (s, 1H), 6.85 (d, ^3J = 7.7 Hz, 2H), 4.09 (m, 2H), 2.98 (s, 3H); ^{13}CNMR (DMSO-d_6): δ_C 48.9, 55.1, 112.3, 116.7, 127.2, 127.4, 128.5, 131.2, 132.1, 134.1, 138.4, 164.2, 165.4, 191.0. Anal. Calcd. for $C_{19}H_{15}BrN_2O_3S_2$: C, 49.25; H, 3.26; N, 6.05. Found: C, 49.71; H, 3.66; N, 6.38.

4.1.20. Z-N-(2,4-Dichlorophenyl)-2-(5-(4-methoxybenzylidene)-4-oxo-2-thioxothiazolidin-3-yl)acetamide 11B

Yellow crystal; yield 75%; m.p. (166–168) °C; IR (KBr, cm^{-1}): 3288, 3048, 2877, 1659, 1522, 1214, 1130; EI-MS (*m/z*, %): 452 (M^+), 453 (M^++1), 454 (M^++2); ^{1}H NMR (400 MHz) (DMSO): δ_H 9.49 (s, 1H), 7.85 (s, 1H), 7.71 (d, ^3J = 7.5 Hz, 1H), 7.56 (d, ^4J = 1.8 Hz, 1H), 7.48 (d, ^3J = 8 Hz, 2H), 7.40 (dd, ^3J = 7.5 Hz, ^4J = 1.8 Hz, 1H), 7.03 (d, ^3J = 8 Hz, 2H), 4.55 (m, 2H), 3.81 (s, 3H); ^{13}CNMR (DMSO-d_6): δ_C 49.6, 55.4, 112.9, 123.7, 127.4, 127.6, 128.5, 129.2, 130.0, 131.6, 132.8, 134.1, 140.3, 157.5, 164.2, 164.9, 191.1; Anal. Calcd. for $C_{19}H_{14}Cl_2N_2O_3S_2$: C, 50.34; H, 3.11; N, 6.18. Found: C,50.72; H, 3.64; N, 6.39.

4.1.21. Z-N-(4-Methoxyphenyl)-2-(5-(4-methoxybenzylidene)-4-oxo-2-thioxothiazolidin-3-yl)acetamide 12B

Reddish brown; yield 66%; M.p. (153–155) °C; IR (KBr, cm^{-1}): 3330, 3100, 2861, 1660, 1559, 1220, 1183; EI-MS (*m/z*, %): 414 (M^+), 415 (M^++1); ^{1}H NMR (400 MHz) (DMSO): δ_H 10.33 (s, 1H), 7.90 (s, 1H), 7.33 (d, ^3J = 7.7 Hz, 2H), 7.19 (d, ^3J = 8 Hz, 2H), 7.11 (d, ^3J = 7.7 Hz, 2H), 6.96 (d, ^3J = 8 Hz, 2H), 4.08 (m, 2H), 3.78 (s, 3H), 3.72 (s, 3H); ^{13}CNMR (DMSO-d_6): δ_C 47.5, 55.3, 112.2, 122.9, 127.2, 128.5, 129.4, 131.2, 134.1, 134.7, 157.5, 160.7, 165.5, 166.7, 189.4; Anal. Calcd. for $C_{20}H_{18}N_2O_4S_2$: C, 57.96; H, 4.38; N, 6.76. Found: C, 58.33; H, 4.84; N, 7.06.

4.1.22. Z-N-(4-Chlorophenyl)-2-(5-(4-methoxybenzylidene)-4-oxo-2-thioxothiazolidin-3-yl)acetamide 13B

Brown, yield 68%; m.p. (160–162) °C; IR (KBr, cm^{-1}): 3343, 3050, 2864, 1657, 1562, 1218, 1140; EI-MS (*m/z*, %): 418 (M^+), 419 (M^++1), 420 (M^++2); ^{1}H NMR (400 MHz) (DMSO): δ_H 10.26 (s, 1H), 7.58 (d, ^3J = 7.7 Hz, 2H), 7.33 (d, ^3J = 7.5 Hz, 2H), 7.25 (d, ^3J = 7.7 Hz, 2H), 7.13 (s, 1H), 6.79 (d, ^3J = 7.5 Hz, 2H), 4.55 (m, 2H), 3.85 (s, 3H); ^{13}CNMR (DMSO-d_6): δ_C 48.9, 55.3, 112.3, 122.6, 127.4, 128.9, 129.5, 132.7, 133.7, 135.1, 139.0, 158.7, 164.1, 165.1, 190.9. Anal. Calcd. for $C_{19}H_{15}ClN_2O_3S_2$: C, 54.48; H, 3.61; N, 6.69. Found: C, 54.91; H, 4.06; N, 6.94.

4.1.23. Z-N-(4-Bromophenyl)-2-(5-(2-hydroxybenzylidene)-4-oxo-2-thioxothiazolidin-3-yl)acetamide 14C

Dark yellow; yield 73%; m.p. (173–175) °C; IR (KBr, cm^{-1}): 3391, 3200, 3088, 2824, 1671, 1573, 1220; EI-MS (*m/z*, %): 448 (M^+), 449 (M^++1), 450 (M^++2); ^{1}H NMR (400 MHz) (DMSO): δ_H 9.99 (s, 1H), 9.85 (s, 1H), 7.91 (s, 1H), 7.79 (d, ^3J = 8 Hz, 2H), 7.62 (d, ^{3} J = 8 Hz, 2H), 7.47–7.02 (m, 4H), 4.63 (m, 2H); ^{13}CNMR (DMSO-d_6): δ_C 49.0, 116.6, 122.1, 127.7, 127.9, 130.9, 131.7, 132.2, 132.6, 136.8, 138.9, 139.3, 157.1, 164.1, 166.2, 190.7. Anal. Calcd. for $C_{18}H_{13}BrN_2O_3S_2$: C, 48.11; H, 2.92; N, 6.23. Found: C, 48.72; H, 3.42; N, 6.69.

4.1.24. Z-N-(2,4-Dichlorophenyl)-2-(5-(2-hydroxybenzylidene)-4-oxo-2-thioxothiazolidin-3-yl)acetamide 15C

Yellowish brown; yield 76%; m.p. (205–207) °C; IR (KBr, cm^{-1}): 3380, 3258, 3044, 2869, 1652, 1553, 1213; EI-MS (*m/z*, %): 438 (M^+), 439 (M^++1), 440 (M^++2); ^{1}H NMR (400 MHz) (DMSO): δ_H 9.92 (s, 1H),

Table 3
Summarized ligand-receptor interactions of **12B** and **15C** towards 4QR6 and 3H4G proteins.

Comp. codes	ALR2 (4QR6)			ALR1 (3H4G)		
12B	−24.11 Kcal/mol	2H-bonds with **His 110**, and **Trp 111**	Two arene-arene with **Tyr 209** and **Trp 111**	−11.2 Kcal/mol	–	One arene-arene with **Trp 22**
15C	−16.43 Kcal/mol	2H-bonds with **His 110**, **Tyr 48**	One arene-arene with **Trp 20**	−11.9 Kcal/mol	–	One arene-arene interaction with **Trp 22**

Bold amino acid residues are the key residues with which the co-crystallized ligands (NADP) interact in both proteins.

9.50 (s, 1H), 7.88 (s, 1H), 7.79 (d, $^{4}J = 1.9$ Hz, 1H), 7.47 (dd, $^{3}J = 7.8$ Hz, $^{4}J = 1.9$ Hz, 1H), 7.29 (d, $^{3}J = 7.8$ Hz, 1H), 6.98–6.68 (m, 4H), 4.63 (m, 2H). ^{13}CNMR (DMSO-d_6): 49.8, 121.7, 123.6, 127.6, 127.8, 129.4, 129.9, 130.2, 131.1, 131.6, 132.4, 136.4, 139.1, 139.7, 157.5, 164.2, 165.1, 190.8. Anal. Calcd. for $C_{18}H_{12}Cl_2N_2O_3S_2$: C, 49.21; H, 2.75; N, 6.38. Found: C, 49.83; H, 3.21; N, 6.85.

4.1.25. Z-N-(4-Methoxyphenyl)-2-(5-(2-hydroxybenzylidene)-4-oxo-2-thioxothiazolidin-3-yl)acetamide 16C

Brown, yield 76%; m.p. (148–150) °C; IR (KBr, cm^{-1}): 3298, 3287, 3100, 2871, 1650, 1582, 1215; EI-MS (*m/z*, %): 400 (M^+), 401 (M^++1); ^{1}H NMR (400 MHz) (DMSO): δ_H 11.41 (s, 1H), 10.20 (s, 1H), 8.16 (s, 1H), 7.97–7.68 (m, 4H), 7.68–7.23 (m, 4H), 3.93 (s, 2H), 3.72 (s, 3H); ^{13}CNMR (DMSO-d_6):δ_C 41.7, 50.9, 111.2, 121.7, 127.9, 128.3, 130.7, 131.6, 132.4, 134.1, 137.2, 139.5, 151.6, 157.2, 162.7, 163.4, 190.2); Anal. Calcd. for $C_{19}H_{16}N_2O_4S_2$: C, 56.99; H, 4.03; N, 7.00. Found: C, 57.55; H, 4.51; N, 7.43.

4.1.26. Z-N-(4-Chlorophenyl)-2-(5-(2-hydroxybenzylidene)-4-oxo-2-thioxothiazolidin-3-yl)acetamide 17C

Dark orange; yield 81%; m.p. (196–198) °C; IR (KBr, cm^{-1}): 3437, 3295, 3050, 2871, 1651, 1589, 1225; EI-MS (*m/z*, %):404 (M^+), 405 (M^++1), 406 (M^++2); ^{1}H NMR (400 MHz) (DMSO): δ_H 9.82 (s, 1H), 9.49 (s, 1H), 7.90 (s, 1H), 7.79–7.47 (m, 4H), 7.38–7.26 (m, 4H), 4.63 (s, 2H); ^{13}CNMR (DMSO-d_6): 48.6, 121.3, 122.1, 127.5, 129.5, 130.7, 131.4, 132.6, 134.4, 135.0, 138.7, 139.6, 157.6, 163.9, 164.9, 190.6. Anal. Calcd. for $C_{18}H_{13}ClN_2O_3S_2$: C, 53.40; H, 3.24; N, 6.92. Found: C, 53.78; H, 3.63; N, 7.41.

4.1.27. Z-N-(4-Bromophenyl)-2-(5-(4-(dimethylamino)benzylidene)-4-oxo-2-thioxothiazolidin-3-yl)acetamide 18D

Orange; yield 71%; m.p. (210–213) °C; IR (KBr, cm^{-1}): 3341, 3070, 2873, 1654, 1578, 1210, 1080; EI-MS (*m/z*, %): 474 (M^+), 475 (M^++1), 476 (M^++2); ^{1}H NMR (400 MHz) (DMSO): δ_H 9.98 (s, 1H), 8.21 (s, 1H), 7.53 (d, $^{3}J = 8$, Hz, 2H), 7.36 (d, $^{3}J = 7.6$, Hz, 2H), 7.21 (d, $^{3}J = 8$, Hz, 2H), 6.85 (d, $^{3}J = 7.6$, Hz, 2H), 4.07 (m, 2H), 3.05 (s, 6H); ^{13}CNMR

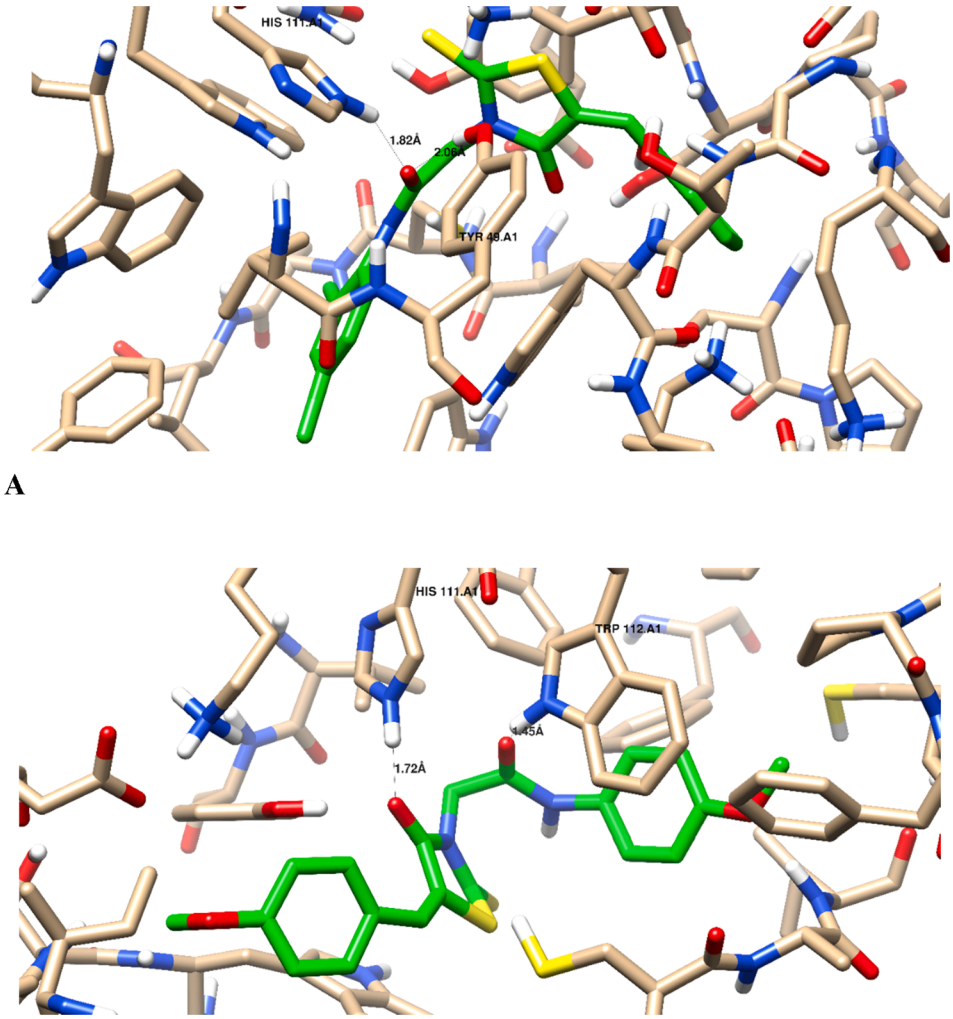

Fig. 3. Three-dimensional representation of compounds **12B** (**A**) and **15C** (**B**) inside the receptor binding site of 4QR6 (ALR2). Compounds are green-colored and H-bonding lengths are represented with dashed lines. (For interpretation of the references to colour in this figure legend, the reader is referred to the web version of this article.)

(DMSO-d_6): 40.1, 49.1, 111.2, 113.2, 127.3, 127.7, 129.1, 131.6, 132.1, 135.2, 138.2, 150.3, 163.6, 164.4, 194.7. Anal. Calcd. for $C_{20}H_{18}BrN_3O_2S_2$: C, 50.53; H, 3.60; N, 8.84. Found: C, 50.75; H, 4.11; N, 9.08.

4.1.28. Z-N-(2,4-Dichlorophenyl)-2-(5-(4-(dimethylamino)benzylidene)-4-oxo-2-thioxothiazolidin-3-yl)acetamide 19D

Dark yellow; yield 70%; m.p. (223–225) °C; IR (KBr, cm^{-1}): 3332, 3075, 2854, 1667, 1599, 1220, 1110; EI-MS (*m/z*, %): 465 (M^+), 466 (M^++1), 467 (M^++2); ^{1}H NMR (400 MHz) (DMSO): δ_H 9.50 (s, 1H), 7.82 (d, ^3J = 7.8 Hz, 1H), 7.70 (s, 1H), 7.49–7.37 (m, 5H), 6.75 (d, ^4J = 1.7 Hz, 1H), 4.22 (m, 2H), 3.15 (s, 6H); ^{13}CNMR (DMSO-d_6): 40.7, 47.6, 112.3, 121.4, 124.8, 126.9, 128.1, 129.2, 129.9, 131.2, 131.6, 135.6, 137.9, 150.1, 164.2, 164.9, 193.7. Anal. Calcd. for $C_{20}H_{17}Cl_2N_3O_2S_2$: C, 51.51; H, 3.67; N, 9.01. Found: C, 51.64; H, 3.83; N, 9.33.

4.1.29. Z-N-(4-Methoxyphenyl)-2-(5-(4-(dimethylamino)benzylidene)-4-oxo-2-thioxothiazolidin-3-yl)acetamide 20D

Dark brown; yield 80%, m.p. (197–199) °C; IR (KBr, cm^{-1}): 3321, 3100, 2871, 1655, 1562, 1214, 1130, 1090; EI-MS (*m/z*, %): 427 (M^+), 428 (M^+ +1); ^{1}H NMR (400 MHz) (DMSO); δ_H 10.10 (s, 1H), 7.83 (s, 1H), 7.47–7.07 (m, 4H), 6.89 (d, ^3J = 8 Hz, 2H), 6.78 (d, ^3J = 7.8 Hz, 2H), 4.61 (m, 2H), 3.79 (s, 3H), 3.23 (s, 6H); ^{13}CNMR (DMSO-d_6): 41.2, 48.9, 54.8, 112.8, 113.2, 122.1, 124.5, 127.2, 131.4, 134.6, 135.2, 150.3, 159.1, 164.7, 165.9, 191.1. Anal. Calcd. for $C_{21}H_{21}N_3O_3S_2$: C, 59.00; H, 4.95; N, 9.83. Found: C, 58.73; H, 4.88; N, 10.28.

4.1.30. Z-N-(4-Chlorophenyl)-2-(5-(4-(dimethylamino)benzylidene)-4-oxo-2-thioxothiazolidin-3-yl)acetamide 21D

Reddish brown; yield 73%; m.p. (202–204) °C; IR (KBr, cm^{-1}): 3275, 3065, 2862, 1710, 1519, 1223, 1155; EI-MS (*m/z*, %): 431 (M^+), 432 (M^+ +1), 433 (M^+ +2); ^{1}H NMR (400 MHz) (DMSO): δ_H 10.21 (s, 1H), 7.52 (d, ^3J = 8 Hz, 2H), 7.30 (d, ^3J = 8 Hz, 2H), 7.20 (d, ^3J = 7.8 Hz, 2H), 7.05 (s, 1H), 6.74 (d, ^3J = 7.8 Hz, 2H), 4.10 (m, 2H), 2.96 (s, 6H); ^{13}CNMR (DMSO-d_6): δ_C 41.6, 47.1, 110.4, 121.7, 127.4, 128.3, 129.7, 131.6, 133.4, 136.1, 139.2, 151.6, 162.7, 163.4, 195.2; Anal. Calcd. for $C_{20}H_{18}ClN_3O_2S_2$: C, 55.61; H, 4.20; N, 9.73. Found: C, 55.81; H, 4.65; N, 10.17.

4.1.31. Z-N-(4-Bromophenyl)-2-(5-(4-nitrobenzylidene)-4-oxo-2-thioxothiazolidin-3-yl)acetamide 22E

Dark red; yield 75%, m.p. (171–173) °C; IR (KBr, cm^{-1}): 3222, 3057, 2873, 1651, 1537, 1525, 1345, 1225; EI-MS (*m/z*, %): 477 (M^+), 478 (M^++1), 479 (M^++2); ^{1}H NMR (400 MHz) (DMSO): δ_H 10.22 (s, 1H), 8.22 (d, ^3J = 7.9 Hz, 2H), 8.08 (d, ^3J = 7.5 Hz, 2H), 7.23 (d, ^3J = 7.9 Hz, 2H), 7.07 (s, 1H), 6.75 (d, ^3J = 7.5 Hz, 2H), 4.08 (m, 2H); ^{13}CNMR (DMSO-d_6): 50.1, 116.0, 124.2, 128.5, 129.9, 131.2, 133.1, 136.4, 139.1, 139.9, 147.2, 166.5, 168.3, 190.8. Anal. Calcd. for $C_{18}H_{12}BrN_3O_4S_2$: C, 45.29; H, 2.32; N, 8.80. Found: C, 45.63; H, 2.74; N, 9.23.

Table 4
Summarized ligand-receptor interactions with 2D and 3D images of the two docked compounds **12B** and **15C** inside the SUR1 protein (6PZ9).

Comp.	SUR1 (6PZ9)		
12B	–22.63 Kcal/mol	2H-bonds with **Asn 437** and **Arg 1248**	One arene-arene with **Tyr 377**
15C	−21.41 Kcal/mol	1H-bond with **Asn 437**	One arene-arene with **Tyr 377**

Bold amino acids are the key residues with which the co-crystallized ligand (Repaglinide) interacts.

Table 5
In silico ADME pharmacokinetics properties of the most active hypoglycemic compounds.

Comp.	Molinspiration 2018.10 [20]						MolSoft [21]			SwissADME [22]
	MWt (D)	MV (A^3)	PSA (A^2)	Log p	nrotb	nviolations	HBA	HBD	Solubility (mg/L)	Drug likeness (Lipinski Pfizer filter)
10B	463.38	341.40	60.34	3.56	5	0	5	1	24.78	"Yes, drug like"MW ≤ 500, Log p ≤ 4.15, HBA ≤ 10 and HDD ≤ 5
11B	453.37	350.59	60.34	4.04	5	0	5	1	4.62	
12B	414.51	349.06	69.57	2.81	6	0	6	1	59.08	
15C	439.35	333.06	71.33	3.92	4	0	5	2	29.75	
16C	400.48	331.54	80.56	2.69	5	0	6	2	146.79	
26F	463.38	341.40	60.34	3.54	5	0	5	1	21.19	
27F	453.37	350.59	60.34	4.01	5	0	5	1	9.0	
Repaglinide	452.6	442.5	78.87	4.87	10	0	4	2	11.38	
Sorbinil	236.2	189.16	67.43	0.86	0	0	3	2	990.63	
Valproic acid	144.21	156.79	37.30	2.80	5	0	2	1	1643.7	

"Mwt: Molecular Weight, MV: Molecular Volume, PSA: Polar Surface Area, Log p: Octanol-water partition coefficient, nrotb: number of rotatable bonds, nviolations: number of violations, HBA: H-Bond Acceptor, HBD: H-Bond Donor" [20,21].

4.1.32. Z-N-(2,4-Dichlorophenyl)-2-(5-(4-nitrobenzylidene)-4-oxo-2-thioxothiazolidin-3-yl)acetamide 23E

Yellow yield; 69%; m.p. (188–190) °C; IR (KBr, cm^{-1}): 3258, 3089, 2860, 1654, 1582, 1550, 1370, 1210; EI-MS (*m/z*, %): 467 (M^+), 468 (M^++1), 469 (M^++2); ^{1}H NMR (400 MHz) (DMSO): δ_H 9.50 (s, 1H), 8.19 (d, ^3J = 8 Hz, 2H), 8.18 (d, ^3J = 8.2 Hz, 1H), 7.82 (d, ^4J = 1.9 Hz, 1H), 7.85 (s, 1H), 7.48 (dd, ^3J = 8.2 Hz, ^4J = 1.9 Hz 1H), 7.40 (d, ^3J = 8 Hz, 2H), 4.45 (m, 2H); ^{13}CNMR (DMSO-d_6): 47.1, 120.3, 121.7, 127.5, 128.1, 128.9, 129.4, 131.1, 133.4, 136.0, 139.2, 140.1, 147.3, 166.7, 168.9, 192.7. Anal. Calcd. for $C_{18}H_{11}Cl_2N_3O_4S_2$: C, 46.16; H, 2.37; N, 8.97. Found: C, 46.42; H, 2.71; N, 9.34.

4.1.33. Z-N-(4-Methoxyphenyl)-2-(5-(4-nitrobenzylidene)-4-oxo-2-thioxothiazolidin-3-yl)acetamide 24E

Yellow; yield 71%; m.p. (162–164) °C; IR (KBr, cm^{-1}): 3380, 3030, 2883, 1690, 1581, 1530, 1360, 1215, 1066; EI-MS (*m/z*, %): 429 (M^+), 430 (M^+ +1); ^{1}H NMR (400 MHz) (DMSO): δ_H 10.65 (s, 1H), 8.27 (d, ^3J = 7.6 Hz, 2H), 7.95 (s, 1H), 7.63 (d, ^3J = 7.8 Hz, 2H), 7.19 (d, ^3J = 7.6 Hz, 2H), 6.97 (d, ^3J = 7.8 Hz, 2H), 4.13 (m, 2H), 3.71 (s, 3H); ^{13}CNMR (DMSO-d_6): δ_C 40.9, 59.7, 117.7, 120.3, 124.5, 133.2, 135.1, 138.4, 140.8, 143.1, 147.2, 160.5, 170.9, 172.8, 191.7. Anal. Calcd. for $C_{19}H_{15}N_3O_5S_2$: C, 53.14; H, 3.52; N, 9.78. Found: C, 53.44; H, 4,06; N, 9.79.

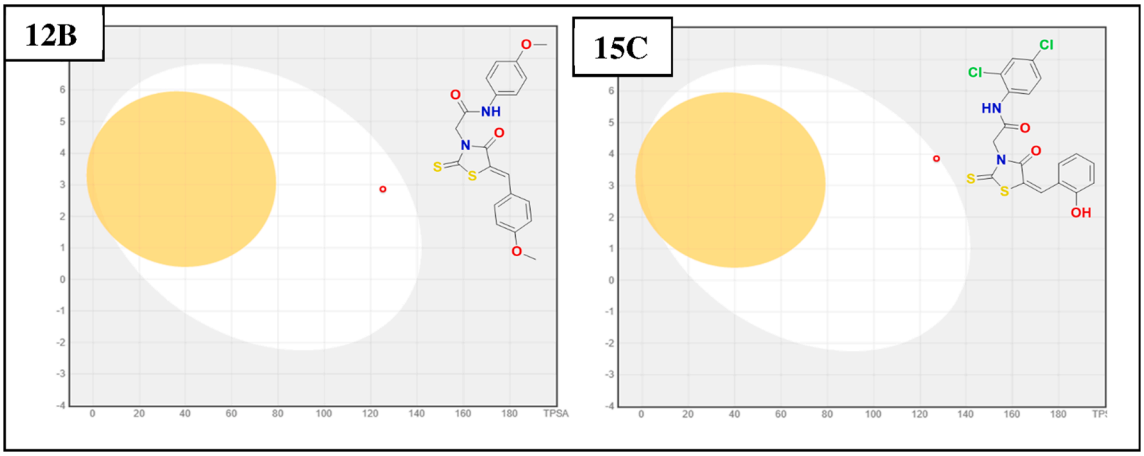

Fig. 4. BOILED-Egg model for compounds **12B** and **15C** using the SwissADME. "Points located in the BOILED-Egg's yolk are molecules predicted to passively permeate through the blood–brain barrier, while points located in the BOILED-Egg's white are molecules predicted to be passively absorbed by gastrointestinal tract".

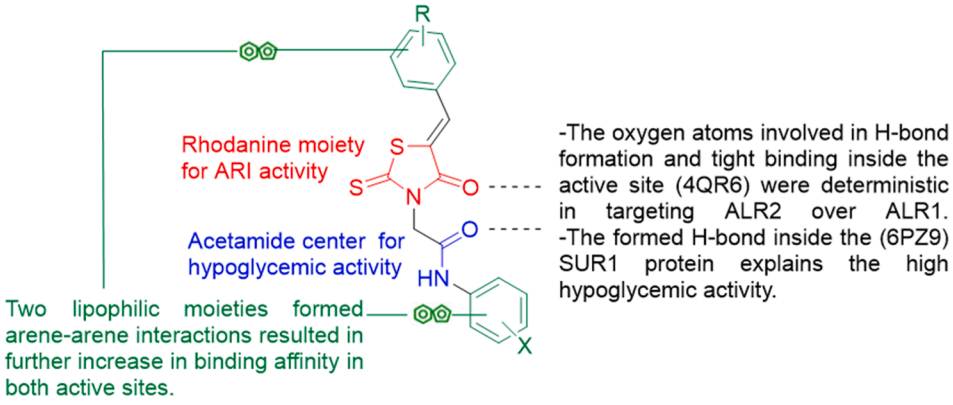

Fig. 5. The observed structure–activity relationships of the designed molecules.

4.1.34. Z-N-(4-Chlorophenyl)-2-(5-(4-nitrobenzylidene)-4-oxo-2-thioxothiazolidin-3-yl)acetamide 25E

Brown; yield 73%; m.p. (174–177) °C; IR (KBr, cm^{-1}): 3265, 3065, 2892, 1699, 1588, 1540, 1350, 1225; EI-MS (*m/z*, %): 433 (M^+), 434 (M^++1), 435 (M^++2); ^{1}H NMR (400 MHz) (DMSO): δ_H 10.70 (s, 1H), 8.28 (d, ^3J = 8.1 Hz, 2H), 7.95 (s, 1H), 7.63 (d, ^3J = 7.9 Hz, 2H), 7.54 (d, ^3J = 8.1 Hz, 2H), 7.32 (d, ^3J = 7.9 Hz, 2H), 4.12 (m, 2H); ^{13}CNMR (DMSO-d_6): δ_C 35.7, 117.8, 126.5, 129.5, 130.3, 131.4, 133.9, 135.1, 139.6, 143.2, 150.1, 172.3, 172.9, 188.5. Anal. Calcd. for $C_{18}H_{12}ClN_3O_4S_2$: C, 49.83; H, 2.79; N, 9.68. Found: C, 50.08; H, 3.08; N, 9.97.

4.1.35. Z-N-(4-Bromophenyl)-2-(5-(3-methoxybenzylidene)-4-oxo-2-thioxothiazolidin-3-yl)acetamide 26F

Dark yellow; yield 77%; m.p. (130–133) °C; IR (KBr, cm^{-1}): 3320, 3020, 2862, 1662, 1536, 1240, 1220; EI-MS (*m/z*, %): 462 (M^+), 463 (M^++1), 464 (M^++2); ^{1}H NMR (400 MHz) (DMSO): δ_H 10.53 (s, 1H), 7.80 (s, 1H) 7.63 (d, ^3J = 8 Hz, 2H), 7.39 (t, ^3J = 7.9 Hz, 1H), 7.22 (d, ^3J = 8 Hz, 2H), 7.08–6.80 (m, 3H), 4.17 (m, 2H), 3.17 (s, 3H); ^{13}CNMR (DMSO-d_6): δ_C 35.4, 60.1, 113.3, 115.6, 117.8, 126.5, 129.5, 130.7, 131.4, 133.9, 135.1, 139.6, 143.2, 150.1, 172.3, 172.9, 187.5; Anal. Calcd. for $C_{19}H_{15}BrN_2O_3S_2$: C, 49.25; H, 3.26; N, 6.05. Found: C, 49.56; H, 3.61; N, 6.37.

4.1.36. Z-N-(2,4-Dichlorophenyl)-2-(5-(3-methoxybenzylidene)-4-oxo-2-thioxothiazolidin-3-yl)acetamide 27F

Orange; yield 75%; m.p. (149–151) °C; IR (KBr, cm^{-1}): 3327, 3098, 2850, 1673, 1547, 1250, 1225; EI-MS (*m/z*, %): 452 (M^+), 453 (M^++1), 454 (M^++2). ^{1}H NMR (400 MHz) (DMSO) δ_H: 9.55 (s, 1H), 7.85 (d, ^3J = 7.6 Hz, 1H), 7.80 (s, 1H) 7.48–7.42 (m, 2H), 7.38 (t, ^3J = 7.8 Hz, 1H), 7.27–7.08 (m, 3H), 4.27 (m, 2H), 3.77 (s, 3H); ^{13}CNMR (DMSO-d_6): δ_C 48.77, 55.1, 113.1, 115.6, 123.7, 125.7, 126.2, 128.9, 129.2, 129.7, 130.0, 131.7, 135.1, 137.2, 141.3, 151.6, 164.9, 169.4, 189.7. Anal. Calcd. for $C_{19}H_{14}Cl_2N_2O_3S_2$: C, 50.34; H, 3.11; N, 6.18. Found: C, 50.67; H, 3.62; N, 6.41.

4.1.37. Z-N-(4-Methoxyphenyl)-2-(5-(3-methoxybenzylidene)-4-oxo-2-thioxothiazolidin-3-yl)acetamide 28F

Yellow; yield 72%; m.p. (115–117) °C; IR (KBr, cm^{-1}): 3317, 3050, 2877, 1655, 1519, 1220, 1205; EI-MS (*m/z*, %): 414 (M^+), 415 (M^++1); ^{1}H NMR (400 MHz) (DMSO): δ_H 10.19 (s, 1H), 7.77 (s, 1H), 7.47 (d, ^3J = 8.1 Hz, 2H), 7.38 (t, ^3J = 7.6 Hz, 1H), 7.27–6.95 (m, 3H), 6.88 (d, ^3J = 8.1 Hz, 2H), 4.51 (m, 2H), 3.82 (s, 3H), 3.79 (s, 3H); ^{13}CNMR (DMSO-d_6): δ_C 48.9, 55.2, 55.4, 113.4, 113.9, 116.6, 122.1, 124.5, 129.6, 130.0, 136.2, 139.2, 140.7, 152.7, 156.6, 166.4, 170.5, 191.2. Anal. Calcd. for $C_{20}H_{18}N_2O_4S_2$: C, 57.96; H, 4.38; N, 6.76; Found: C, 58.23; H, 4.85; N, 7.10.

4.1.38. Z-N-(4-Chlorophenyl)-2-(5-(3-methoxybenzylidene)-4-oxo-2-thioxothiazolidin-3-yl)acetamide 29F

Yellow; yield 69%; m.p. (127–129) °C; IR (KBr, cm^{-1}): 3344, 3100, 2960, 1660, 1536, 1235, 1200; EI-MS (*m/z*, %): 418 (M^+), 419 (M^++1), 420 (M^++2); ^{1}H NMR (400 MHz) (DMSO): δ_H 10.55 (s, 1H), 7.85 (s, 1H), 7.63–7.38 (m, 4H), 7.38 (t, ^3J = 8.2 Hz, 1H), 7.06–6.91 (m, 3H), 4.13 (m, 2H), 3.75 (s, 3H); ^{13}CNMR (DMSO-d_6): δ_C 49.6, 55.2, 112.2, 115.6, 121.3, 122.5, 126.2, 129.2, 129.4, 135.4, 137.5, 140.3, 142.3, 157.6,

166.2, 168.5, 191.1. Anal. Calcd. for $C_{19}H_{15}ClN_2O_3S_2$: C, 54.48; H, 3.61; N, 6.69. Found: C, 54.90; H, 3.87; N, 7.05.

4.1.39. Z-N-(4-Bromophenyl)-2-(5-(3-bromobenzylidene)-4-oxo-2-thioxothiazolidin-3-yl)acetamide 30G

Brown; Yield 78%; m.p. (259–260) °C; IR (KBr, cm^{-1}): 3290, 3066, 2870, 1654, 1580, 1220; EI-MS (*m/z*, %): 510 (M^+), 511 (M^++1), 512 (M^++2); ^{1}H NMR (400 MHz) (DMSO); δ_H 10.51 (s, 1H), 8.19 (s, 1H), 7.87–7.40 (m, 4H), 7.36 (t, ^3J = 7.5 Hz, 1H), 7.21–7.06 (m, 3H), 4.10 (m, 2H); ^{13}CNMR (DMSO-d_6): δ_C 49.0, 116.7, 122.5, 127.4, 129.4, 130.0, 132.1, 138.2, 139.4, 139.8, 141.2, 143.6, 147.6, 164.3, 166.5, 191.1. Anal. Calcd. for $C_{18}H_{12}Br_2N_2O_2S_2$: C, 42.21; H, 2.36; N, 5.47. Found: C, 42.73; H, 2.61; N, 5.89.

4.1.40. Z-N-(2,4-Dichlorophenyl)-2-(5-(3-bromobenzylidene)-4-oxo-2-thioxothiazolidin-3-yl)acetamide 31G

Dark yellow**,** yield 73%, m.p, (127–129) °C; IR (KBr, cm^{-1}): 3394, 3059, 2855, 1663, 1585, 1217; EI-MS (*m/z*, %): 500 (M^+), 501 (M^++1), 502 (M^++2); ^{1}H NMR (400 MHz) (DMSO): δ_H 9.78 (s, 1H), 7.78 (d, ^3J = 8 Hz, 1H), 7.70 (s, 1H), 7.68 (t, ^3J = 7.7 Hz, 1H), 7.54–7.48 (m, 3H), 7.43–7.39 (m, 2H), 4.55 (m, 2H); ^{13}CNMR (DMSO-d_6): δ_C 49.6, 122.7, 123.4, 128.5, 129.0, 129.2, 129.9, 127.6, 131.6, 134.6, 134.9, 139.6, 141.6, 142.6, 143.8, 149.2, 163.3, 164.9, 195.2. Anal. Calcd. for $C_{18}H_{11}BrCl_2N_2O_2S_2$: C, 43.05; H, 2.21; 14.12; N, 5.58. Found: C, 43.47; H, 2.55; N, 5.87.

4.1.41. Z-N-(4-Methoxyphenyl)-2-(5-(3-bromobenzylidene)-4-oxo-2-thioxothiazolidin-3-yl)acetamide 32G

Yellow; yield 76%; m.p. (187–188) °C, IR (KBr, cm^{-1}): 3275, 3090, 2862, 1660, 1541, 1250, 1225; EI-MS (*m/z*, %): 462 (M^+), 463 (M^++1), 464 (M^++2); ^{1}H NMR (400 MHz) (DMSO): δ_H 9.96 (s, 1H), 7.88 (s, 1H), 7.70–7.55 (m, 3H), 7.46 (d, ^3J = 7.9 Hz, 2H), 7.32 (t, ^3J = 7.4 Hz, 1H), 6.89 (d, ^3J = 7.9 Hz, 2H), 4.63 (m, 2H), 3.71 (s, 3H); ^{13}CNMR (DMSO-d_6): δ_C 48.7, 55.6, 113.9, 121.1, 122.4, 129.3, 132.1, 134.7, 135.9, 139.6, 140.8, 142.8, 147.2, 156.6, 164.2, 165.4, 195.2. Anal. Calcd. for $C_{19}H_{15}BrN_2O_3S_2$: C, 49.25; H, 3.26; N, 6.05. Found: C, 49.72; H, 3.54; N, 6.42.

4.1.42. Z-N-(4-Chlorophenyl)-2-(5-(3-bromobenzylidene)-4-oxo-2-thioxothiazolidin-3-yl)acetamide 33G

Yellow; yield 78%; m.p. (273–275) °C; IR (KBr, cm^{-1}): 3340, 3090, 2840, 1685, 1598, 1220; EI-MS (*m/z*, %): 466 (M^+), 467 (M^++1), 468 (M^++2); ^{1}H NMR (400 MHz) (DMSO): δ_H 10.52 (s, 1H), 8.13 (s, 1H), 7.80 (d, ^3J = 8 Hz, 2H), 7.64–7.53 (m, 4H), 7.35 (d, ^3J = 8 Hz, 2H), 4.13 (m, 2H); ^{13}CNMR (DMSO-d_6): δ_C 48.1, 122.7, 127.4, 128.5, 129.7, 132.6, 134.8, 136.5, 139.8, 142.7, 146.2, 151.6, 155.2, 162.7, 163.4, 195.3; Anal. Calcd. for $C_{18}H_{12}BrClN_2O_2S_2$: C, 46.22; H, 2.59; N, 5.99. Found: C, 46.81; H, 2.77; N, 6.54.

4.2. Biological evaluation

"The *in-vivo* hypoglycemic activities of target compounds as well as their *in-vitro* inhibitory activities against both ALR1 and ALR2 followed our published procedures [33]. Both ALR enzymes were purchased from BioVision, Incorporated [34]. The experimental protocols were approved by The Ethics Committee of the Suez Canal University"

4.3. Molecular docking study

The X-ray crystal structures of three proteins with the co-crystallized ligands; SUR 1 membrane protein (PDB ID: 6PZ9), ALR1 (PDB ID: 3H4G), and ALR2 (PDB ID: 4QR6) were downloaded from the Protein Data Bank. Protein structure were optimized by adjusting the amino acids with missing atoms or alternative positions, and ligand structures were built, optimized, and energetically favored using Maestro. "Molecular docking simulation studies was performed on Molecular Operating Environment (MOE®, 8) version 2016 [35]". Molecular docking study was carried following the routine work [36] of preparation of the appropriate formats of receptor and ligands, determination of grid box dimensions box of 10 Å in the x, y and z directions centered on the ligand, and finally docking with binding activities in terms of binding energies and ligand-receptor interactions. Chimera was used to analyze the binding disposition and interactive analysis.

4.4. Bioinformatics study

"Bioinformatics study of the novel compounds were computed using Molinspiration, [20], SwissADME [22] website and MolSoft software [37,38]".

5. Conclusion

Diabetes Mellitus (DM) is a chronic and complex illness characterized by hyperglycemia that arises from impaired pancreatic function. Although various treatments for diabetes mellitus are presented, diabetic patients still suffer from serious complications. These complications are directly related to ALR2 activity while its analogue ALR1 is a useful enzyme. Therefore, the non-selective inhibition of both ALR enzymes leads to serious toxicity. Our aim was to develop hypoglycemic agents as well as potent and selective inhibitors of ALR2 with minimal side effects. The synthesis of the novel compounds was accomplished throughout simple chemical pathways. Series **A** of the target compounds included acetamide derivatives of unsubstituted-5-benzylidenerhodanine**.** Furthermore, various *o*-, *m*- and *p*-substituents decorated the 5-benzylidenerhodanine moiety in series **C, F, G, B, D** and **E**. Most of the novel compounds displayed promising hypoglycemic activities as well as selective ALR2 inhibition with IC_{50} values in the low micro molar-range. Regarding *in-vivo* hypoglycemic activity, the most active newly synthesized compounds were **10B, 11B, 12B, 15C, 16C, 26F** and **27F** with 80.7, 85.2, 87, 82.3, 83.5, 81.4 and 85.3% reduction in blood glucose respectively. They were more active than repaglinide with 65.4% reduction. Concerning *in-vitro* aldose reductase inhibitory activity, the most potent compounds were **12B** and **15C** and **11B** with an IC_{50} values of 0.29, 0.35, and 0.43 μM, respectively. Compounds **12B** and **15C** were more potent than epalrestat with IC_{50} value 0.40 μM. The selectivity indices of compounds **12B** and **15C** towards ALR2 were 134 and 116 folds, respectively. Docking studies gave partial explanation for the binding mode of the most active compounds **12B** and **15C** in *B*-cell SUR1 membrane protein and ALR2 active site particularly the specificity pocket (localized between Trp111 and Leu300) [39]. Molecular docking revealed that the introduction of *o*- or *p*-substituents, containing an oxygen atom (hydroxy or methoxy groups) on benzylidene moiety, might promote ALR2 inhibition and hypoglycemic activities of the target compounds. Moreover, the flexibility (acceptable number of rotatable bonds) of the target compounds increases their ALR2 inhibitory activity. Therefore, the recent study might open new avenues to consider these ligands for further development not only as hypoglycemic agents but also as potent and selective inhibitors of ALR2 with minimal side effects.

CRediT authorship contribution statement

Manar G. Salem: Experimental section. **Yasmine M. Abdel Aziz:** Conceptualization, Supervision, Writing - original draft, Writing - review & editing. **Marwa Elewa:** Conceptualization, Supervision, Writing - original draft, Writing - review & editing. **Mohamed S. Nafie:** Docking and bioinformatics studies. **Hosam A. Elshihawy:** Conceptualization, Supervision. **Mohamed M. Said:** Conceptualization, Supervision.

Declaration of Competing Interest

The authors declare that they have no known competing financial

interests or personal relationships that could have appeared to influence the work reported in this paper.

Acknowledgment

We would like to thank Dr. Waled Ali (Biochemistry Department, Faculty of Pharmacy, Cairo University) for the biological evaluation. The authors declare no potential conflicts of interest. This study did not receive any grant from funding agencies in the commercial, public , or not-for-profit sectors.

Appendix A. Supplementary data

Supplementary data to this article can be found online at https://doi.org/10.1016/j.bioorg.2021.104909.

References

[1] T. Uzu, T. Harada, M. Sakaguchi, M. Kanasaki, K. Isshiki, S. Araki, T. Sugiomoto, D. Koya, M. Haneda, A. Kashiwagi, Glucocorticoid-induced diabetes mellitus: prevalence and risk factors in primary renal diseases, Nephron Clin. Pract. 105 (2) (2007) c54–c57.
[2] J. Deruiter, Overview of the antidiabetic agents, Endocrine Pharmacother. Module 3 (3) (2003) 45–50.
[3] M.G. Salem, Y.M.A. Aziz, M. Elewa, H.A. Elshihawy, M.M. Said, Synthesis and molecular modeling of novel non-sulfonylureas as hypoglycemic agents and selective ALR2 inhibitors, Bioorg. Med. Chem. (2019).
[4] S.J. Elder, A.H. Lichtenstein, A.G. Pittas, S.B. Roberts, P.J. Fuss, A.S. Greenberg, M. A. McCrory, T.J. Bouchard, E. Saltzman, M.C. Neale, Genetic and environmental influences on factors associated with cardiovascular disease and the metabolic syndrome, J. Lipid Res. 50 (9) (2009) 1917–1926.
[5] O. El-Kabbani, F. Ruiz, C. Darmanin, R.-T. Chung, Aldose reductase structures: implications for mechanism and inhibition, Cell. Mol. Life Sci. CMLS 61 (7–8) (2004) 750–762.
[6] S. Miyamoto, Recent advances in aldose reductase inhibitors: potential agents for the treatment of diabetic complications, Expert Opin. Ther. Pat. 12 (5) (2002) 621–631.
[7] H. Andleeb, Y. Tehseen, F. Jabeen, I. Khan, J. Iqbal, S. Hameed, Exploration of thioxothiazolidinone–sulfonate conjugates as a new class of aldehyde/aldose reductase inhibitors: A synthetic and computational investigation, Bioorg. Chem. 75 (2017) 1–15.
[8] M. Taha, Mixing Pharmacophore Modeling and Classical QSAR Analysis as Powerful Tool for Lead Discovery, Virtual Screen. 1 (2012).
[9] T.N. Reddy, M. Ravinder, P. Bagul, K. Ravikanti, C. Bagul, J.B. Nanubolu, K. Srinivas, S.K. Banerjee, V.J. Rao, Synthesis and biological evaluation of new epalrestat analogues as aldose reductase inhibitors (ARIs), Eur. J. Med. Chem. 71 (2014) 53–66.
[10] Z. Iqbal, S. Hameed, S. Ali, Y. Tehseen, M. Shahid, J. Iqbal, Synthesis, characterization, hypoglycemic and aldose reductase inhibition activity of arylsulfonylspiro [fluorene-9, 5′-imidazolidine]-2′, 4′-diones, Eur. J. Med. Chem. 98 (2015) 127–138.
[11] Y.P. Agrawal, M.Y. Agrawal, A.K. Gupta, Design, synthesis and evaluation of Rhodanine derivatives as aldose reductase inhibitors, Chem. Biol. Drug Des. 85 (2) (2015) 172–180.
[12] R. Guardado-Mendoza, A. Prioletta, L.M. Jiménez-Ceja, A. Sosale, F. Folli, The role of nateglinide and repaglinide, derivatives of meglitinide, in the treatment of type 2 diabetes mellitus, Arch. Med. Sci.: AMS 9 (5) (2013) 936.
[13] Y.M.A. Aziz, M.M. Said, H.A. El Shihawy, K.A. Abouzid, Discovery of novel tricyclic pyrido [3′, 2′: 4, 5] thieno [3, 2-d] pyrimidin-4-amine derivatives as VEGFR-2 inhibitors, Bioorg. Chem. 60 (2015) 1–12.
[14] T.J. Reilly, The preparation of lidocaine, J. Chem. Ed. 76 (11) (1999) 1557.
[15] A.M. Qandil, L.I. Fakhouri, a-Anilinoketones, Esters and Amides: A Chemical Study, Pharmaceuticals 5 (6) (2012) 591–612.
[16] M. Stefek, V. Snirc, P.-O. Djoubissie, M. Majekova, V. Demopoulos, L. Rackova, Z. Bezakova, C. Karasu, V. Carbone, O. El-Kabbani, Carboxymethylated pyridoindole antioxidants as aldose reductase inhibitors: Synthesis, activity, partitioning, and molecular modeling, Bioorg. Med. Chem. 16 (9) (2008) 4908–4920.
[17] C.A. Lipinski, Lead-and drug-like compounds: the rule-of-five revolution, Drug Discov. Today: Technol. 1 (4) (2004) 337–341.
[18] D.E. Clark, S.D. Pickett, Computational methods for the prediction of 'drug-likeness', Drug Discov. Today 5 (2) (2000) 49–58.
[19] D.F. Veber, S.R. Johnson, H.-Y. Cheng, B.R. Smith, K.W. Ward, K.D. Kopple, Molecular properties that influence the oral bioavailability of drug candidates, J. Med. Chem. 45 (12) (2002) 2615–2623.
[20] M.S. Nafie, A.M. Amer, A.K. Mohamed, E.S. Tantawy, Discovery of novel pyrazolo [3, 4-b] pyridine scaffold-based derivatives as potential PIM-1 kinase inhibitors in breast cancer MCF-7 cells, Bioorg. Med. Chem. 115828 (2020).
[21] E. Youssef, M. El-Moneim, W. Fathalla, M.S. Nafie, Design, synthesis and antiproliferative activity of new amine, amino acid and dipeptide-coupled benzamides as potential sigma-1 receptor, J. Iran. Chem. Soc 1–18 (2020).
[22] A. Daina, O. Michielin, V. Zoete, SwissADME: a free web tool to evaluate pharmacokinetics, drug-likeness and medicinal chemistry friendliness of small molecules, Sci. Rep. 7 (2017) 42717.
[23] P.G. Baraldi, D. Preti, M.A. Tabrizi, F. Fruttarolo, G. Saponaro, S. Baraldi, R. Romagnoli, A.R. Moorman, S. Gessi, K. Varani, N 6-[(hetero) aryl/(cyclo) alkyl-carbamoyl-methoxy-phenyl]-(2-chloro)-5′-N-ethylcarboxamido-adenosines: the first example of adenosine-related structures with potent agonist activity at the human A 2B adenosine receptor, Bioorg. Med. Chem. 15 (7) (2007) 2514–2527.
[24] L. Ma, S. Li, H. Zheng, J. Chen, L. Lin, X. Ye, Z. Chen, Q. Xu, T. Chen, J. Yang, Synthesis and biological activity of novel barbituric and thiobarbituric acid derivatives against non-alcoholic fatty liver disease, Eur. J. Med. Chem. 46 (6) (2011) 2003–2010.
[25] Z. Aktürk, F. Kılıç, K. Erol, V. Pabuçcuoğlu, Synthesis and anticonvulsant activity of some ω-(1H-1-imidazolyl)-N-phenylalkanoic acid amide derivatives, Il Farmaco 57 (3) (2002) 201–206.
[26] S.Q. Tang, Y.Y.I. Lee, D.S. Packiaraj, H.K. Ho, C.L.L. Chai, Systematic evaluation of the metabolism and toxicity of thiazolidinone and imidazolidinone heterocycles, Chem. Res. Toxicol. 28 (10) (2015) 2019–2033.
[27] L. Saliyeva, A. Grozav, N. Yakovychuk, N.Y. Slyvka, M. Vovk, Synthesis, the antifungal and antibacterial activity of N1-substituted N2-(4, 5-dihydro-1, 3-thiazol-2-yl) glycinamides, Žurnal organìčnoï ta farmacevtičnoï hìmìï 15 (3(59)) (2017) 55–60.
[28] D.N. Pansare, Development of novel inhibitors of bacterial enzyme mur b, 2016.
[29] V. Opletalova, J. Dolezel, K. Kralova, M. Pesko, J. Kunes, J. Jampilek, Synthesis and characterization of (Z)-5-arylmethylidene-rhodanines with photosynthesis-inhibiting properties, Molecules 16 (6) (2011) 5207–5227.
[30] S. Jadhav, M. Shioorkar, O. Chavan, A. Sarkate, D. Shinde, R. Pardeshi, Alum [KAl (SO4) 2• 12H2O] catalyzed microwave assisted synthesis of 5-arylidine-2-(methylthio)-thiazolone derivatives in water, Eur. J. Chem. 6 (4) (2015) 410–416.
[31] D.D. Subhedar, M.H. Shaikh, L. Nawale, A. Yeware, D. Sarkar, B.B. Shingate, [Et 3 NH][HSO 4] catalyzed efficient synthesis of 5-arylidene-rhodanine conjugates and their antitubercular activity, Res. Chem. Intermed. 42 (8) (2016) 6607–6626.
[32] D.N. Pansare, R.N. Shelke, D.B. Shinde, A Facial Synthesis and Anticancer Activity of (Z)-2-((5-(4-nitrobenzylidene)-4-oxo-4, 5-dihydrothiazol-2-yl) amino)-substituted Acid, J. Heterocycl. Chem. 54 (6) (2017) 3077–3086.
[33] M.G. Salem, Y.M.A. Aziz, M. Elewa, H.A. Elshihawy, M.M. Said, Molecular modelling and synthesis of spiroimidazolidine-2, 4-diones with dual activities as hypoglycemic agents and selective inhibitors of aldose reductase, Bioorg. Chem. 79 (2018) 131–144.
[34] I. BioVision, EZDetect™ Aldo-keto Reductase Activity Assay Kit, Colorimetric.
[35] Chemical Computing Group Inc. MO Canada, Molecualr Operating Environment (MOE), 2016. www.chemcomp.com.
[36] M.S. Nafie, M.A. Tantawy, G.A. Elmgeed, Screening of different drug design tools to predict the mode of action of steroidal derivatives as anti-cancer agents, Steroids 152 (2019), 108485.
[37] M.A. Koch, A. Schuffenhauer, M. Scheck, S. Wetzel, M. Casaulta, A. Odermatt, P. Ertl, H. Waldmann, Charting biologically relevant chemical space: a structural classification of natural products (SCONP), PNAS 102 (48) (2005) 17272–17277.
[38] S. Agnihotri, R. Narula, K. Joshi, S. Rana, M. Singh, In silico modeling of ligand molecule for non structural 3 (NS3) protein target of flaviviruses, Bioinformation 8 (3) (2012) 123.
[39] I. Crespo, J. Giménez-Dejoz, S. Porté, A. Cousido-Siah, A. Mitschler, A. Podjarny, H. Pratsinis, D. Kletsas, X. Parés, F.X. Ruiz, Design, synthesis, structure-activity relationships and X-ray structural studies of novel 1-oxopyrimido [4, 5-c] quinoline-2-acetic acid derivatives as selective and potent inhibitors of human aldose reductase, Eur. J. Med. Chem. 152 (2018) 160–174.